hydralab+ Adaptation for Climate Change

JRA 2 COMPLEX (Cross disciplinary Observations of Morphodynamics and Protective structures, Linked to Ecology and eXtreme events)

Guidelines for mobile bed tests with mixed sedimentary substrates

Deliverable 9.2

Status: Final

Version: 1

Date: November 2017

EC contract no 654110, HYDRALAB+

DOCUMENT INFORMATION

Title	Guidelines for mobile bed tests with mixed sedimentary substrates
Lead Author	Iván Cáceres
Contributors	All COMPLEX partners
Distribution	Public
Document Reference	Deliverable D9.2

DOCUMENT HISTORY

Date	Revision	Prepared by	Organisation	Approved by	Status
October 2017		Iván Cáceres and Agustín Sánchez-Arcilla	Universitat Politècnica de Catalunya		Draft
18/11/2017	V1	Iván Cáceres and Agustín Sánchez-Arcilla	Universitat Politècnica de Catalunya	Frans Hamer	Final

ACKNOWLEDGEMENT

The work described in this publication was supported by the European Community's Horizon 2020 Programme through the grant to the budget of the Integrated Infrastructure Initiative HYDRALAB+, Contract no. 654110.

DISCLAIMER

CONTENTS

LIST OF FIGURES

LIST OF TABLES

1 EXECUTIVE SUMMARY

Mobile bed tests are a unique tool for addressing the complex issue of sediment transport and associated morphological evolution under different sediment sizes. The strongly non–linear relations between hydraulic drivers and grain sizes preclude numerical models for providing a reliable answer within the present state of the art. The strong spatial and temporal variability limit the general application of field measurements, given the limits of resolution and coverage usual in field campaigns, which hamper the derivation of more general conclusions.

Within this framework, deliverable 9 II considers the present state of the art in terms of grain parameters, transport mechanisms and formulations and incipient motion conditions. From here some considerations on present sources of error when calculating transport are discussed. This leads to some considerations on how to apply these limits to hydraulic models, including the design and interpretation of experiments.

The second chapter of the deliverable deals with the multiple scale feedbacks between hydrodynamics and sediment transport, including the interactions with bed forms and geometry for bi-modal sediment mixes. The state of the art and applicable formulations for ripples are discussed next, illustrated by the criteria selected to design the large scale test with mixed sediments in the Barcelona flume.

The range of wave conditions should be determined from the simultaneous consideration of flume performance capabilities and the ripple regime desirable, leading to a more general applicability of the proposed approach.

The next block of the deliverable discusses the settings, deployment and sampling policy for the instrumentation, again illustrated for the large scale flume test in Barcelona with mixed sediments. This is followed by an overview of some initial results, looking for commonalities and differences between unimodal and mixed sediments.

The deliverable ends with some conclusions on the potential of large scale facilities for mixed sediments and the importance of these sedimentary deposits under present conditions but especially under future climates.

2 SOME INTRODUCTORY REMARKS ON SEDIMENT FLUXES FOR HYDRAULIC TESTS

The two main uncertainties or constraints affecting sediment transport estimations are:

- The spatial and temporal variability of the transport processes
- The sparse information available from measurements (lab or field) particularly for bed material transport
- The strongly nonlinear relation between hydraulic drivers and grain size (and thus transport rate).

The large variability demands a large enough number of observation points, which combined with the nonlinear steep relation controlling transport, results in estimates of limited accuracy, particularly when averaged in spatial and temporal terms.

The limitations in field campaigns suggest the important role that laboratory models can play in this area, particularly for a mix of sediment sizes, where sediment supply and transport rates will interact in a nonlinear manner with the composition and topography of the sea bed.

2.1 GRAIN PARAMETERS

The sediment diameter and weight affect its mobility directly. In addition, when there is a mix of sizes the smaller grains will become less mobile than they would be in a uniform sized bed. Conversely the larger grains will be easier to move in the mixture. This is the relative size effect, documented in many previous works (e.g. Church and Hassan, 2002; Wilcock et al, 2009; Kostaschuk et al, 2005; Eidsvik et al, 2004 and Wheaton et al, 2010).

The mix of sediments can be conceived as a three dimensional framework formed by the coarser sediment, where the inter spaces may be empty or contain finer sediments. For instance, when thinking of a sand-gravel mixture, common enough in beaches and rivers, when the proportion of sand is smaller than 0.25, the sedimentary deposit is called a framework supported bed, since it is the gravel particles that constitute the framework supporting the deposit. When the proportion of sand is larger than 0.4, the larger grains are supported by a matrix of finer sediment and therefore this is called a matrix supported deposit.

The question of which is the characteristic sediment whether it is that found on the bed surface or slightly below is another important conundrum. The subsurface sediment has been shown (see e.g. Church and Hassan 2002) to be more directly related to the transported load. This situation can be described as a pavement or mobile armour (e.g. Parker and Klingeman 1982) where a relatively coarser surface layer forms above the sub-surface make fewer fine particles available for transportation. Hence, although the finer particles are easier to transport, with less fine particles being available the transport load size distribution is found to be equivalent to the subsurface grain size distribution. It is because of this, that the substrate size distribution is normally the most appropriate for characterising sediment size used transport formulations.

However, the composition of the bed surface below any flow will depend on the antecedent conditions of sediment supply and hydrodynamic drivers. The surface therefore does not only depend on the direct hydrodynamics acting on it but also on the pre-existing bed morphology and sediment supply. Despite these considerations and in the absence of sufficient data on the subsurface sediments many surface based transport formulas are nowadays applied, introducing potentially significant uncertainties into the calculations.

In flow conditions which exceed the threshold of motion a mobile sediment bed will develop bedforms whose height and length depend on the sediment grain sizes and the flow velocities. At high velocities these bedforms are washed out and sediment is transported as so-called sheet flow in a thin layer above the bed. For uniform sediment under wave conditions the mobility number Ψ_w can be used as an indicator for the transport regime:

$$\Psi_w = \frac{u_w^2}{(s-1)gD_{50}}$$

with

$$u_w = \sqrt{0.5\hat{u}_{on}^2 + 0.5\hat{u}_{off}^2}$$

where D_{50} is the median grain diameter, $s = \rho_s/\rho_w$ is the relative sand density (with sand density ρ_s and water density ρ_w), g is the gravitational constant and u_w is the equivalent sinusoidal orbital velocity amplitude in terms of u_{rms} for second-order Stokes orbital flows. While ripple conditions prevail for $\Psi_w < 100$ (i.e. at lower orbital velocities), sheet-flow conditions, i.e. a flat bed, prevail for $\Psi_w > 100$, as the bedforms are washed out at higher orbital velocities.

2.2 TRANSPORT MECHANISMS

Sediment transport is frequently an intermittent process, highly variable in space and time. The transport rates measured in the field and also in large flume tests (both under waves and unidirectional flow) show a number of energetic events or transporting events, which produce significant pulses of sediment transport (e.g. Iseya and Ikeda, 1987). The remaining time sediment transport rates decrease sharply.

Sediment transport has been conventionally split between bed load (sliding, rolling or hopping grains) and suspended load (picked up off the bed and suspended in the water column by turbulence). Coarser grains are normally transported as bed load while the finer ones are transported as suspended load. Depending on the source of the grain, the classification is sometimes into bed material load and wash material load, referring to grains found in the sea bed or grains found mainly in the water column. The distinction between both modes of transport is not sharp and may be difficult to determine in some experiments.

The supply of sediment will also affect the transport of all sediment sizes. For instance, increasing the sand content increases the fractional transport rate of sand but also that of the coarser material (Wilcock et al. 2001). This means that changing the sediment supply for one fraction will affect all transport rates, for all sediment sizes.

It is because of these complexities the transport models are still incomplete and therefore more direct observations are needed, relating the transport to the sediment supply. This is particularly important since any imbalance between transport capacity and sediment supply will result in erosion or deposition from the flume bed.

Any minor changes in sediment storage will also influence transport rates. This results in spatial variations, such as when carrying out flume tests with different sediment sizes, it will affect the observed sediment transport rates and also the grain size distribution of the transported sediment. This is particularly important when the hydro-morphodynamic conditions are not in equilibrium so that sediment transport composition may be changing substantially during an experiment.

For example, bedforms continually adjust in natural flows that are frequently non-uniform (in space) and unsteady (in time). The rates bedform adjustment and the necessary adjustment in sediment

transport rates will differ in response to changes in hydrodynamics (increasing or decreasing shear stress) as well as pre-existing bedforms (increasing or decreasing bedform size and/or asymmetry).

2.3 TRANSPORT FORMULATIONS

In terms of the underlying physical processes the most commonly employed transport formulae express the transport rate as a proportionality coefficient times the excess of shear stress with respect to a threshold. This shear stress is normally written in dimensionless terms, dividing the actual shear by the specific submerged weight times the diameter. The dimensionless transport parameter is normally divided by a reference shear stress to the power 3/2 and it is this dimensionless transport that it is employed to determine the initiation of motion which is referred to a small percentage of sand grains in motion (0.2% as a reference) rather than referring it to the individual motion of sand grains.

For mixed sediment distributions it is normally assumed that the function defined for uniform size sediment can also be applied, in terms of a median sediment diameter, D50. This does not allow the explicit estimation of changes in transport grain size and it is based on the assumption that such transport does not vary with sediment diameter.

More advanced formulations assume that the transport rate for a given fraction of sediment is proportional to the Shields number for that fraction and that changes in one fraction are not influenced by the rest of fractions. This is clearly inconsistent the observed experience where the finer fractions move with more difficulty in the presence of the coarser fractions and the coarser fractions move more easily in the presence of the finer fractions.

2.4 INCIPIENT MOTION

This topic, difficult in itself for uniform size sediments, becomes even more complex for mixed sediment sizes. It can be related to a threshold in a sediment transport formulation or to a reference level of transport, measured or inferred from the observations.

For uniform sized sediment the transport rate depends on bed geometry, fluid and sediment characteristics and hydraulic available power. The observed behaviour that larger sediment sizes move more easily in the presence of a smaller grains and conversely, smaller grains becoming harder to move in the presence of a large grain bed, cannot be introduced easily into the available knowledge of formulations for incipient motion of mixed sediment sizes. In flume studies of fluvially transported sediment, mixed grain size beds are shown to give rise to more complex bed structures such that individual grains may be relatively easier or more difficult to entrain depending on both their size and position relative to other grains. These bed structuring effects alter the projection of particles into the flow and the pivoting angles required to exceed the threshold for entrainment (e.g. Komar and Li, 1989). This leads to hiding of small grains and a relative reduction in their mobility and, in contrast, relatively larger grains may be more exposed and relatively easier to transport than their size would suggest.

The common assumption is that all sizes have about the same reference value for the critical threshold in shear stress. This leads to the apparent paradox of how to combine the absolute size effect (finer grains move more easily) and the relative size effect just described.

For bimodal distributions of sediment sizes, it is usual to treat them as composed of two fractions and to model each fraction with specific formulations.

The problems are related to the actual bed composition (and the implications for bed geometry) which under goes a transition as a function of sediment transport and the pre-existing bed geometry, including the upper sediment layer. The transition from a framework supported sedimentary deposit (where the bed consists essentially of the coarser sediments) to a matrix supported bed (which is in this case formed by the finer grains in which there are floating coarser particles) is difficult to deal with and represents a challenge in transport patterns and therefore formulations. This is complicated by the nonlinear relation between transport rate and bed shear stress and it may lead to large errors in sediment transport predictions from small uncertainties in bed composition or structure.

2.5 SOURCES OF ERROR IN TRANSPORT ASSESSMENTS

The commonly employed sediment transport formulations depend on the dimensionless shear stress to a power of about 3/2. The dimensionless shear stress is calculated as the actual shear stress divided by the specific submerged weight times the diameter. This means that the uncertainty appears from a) the acting shear stress, and b) the actual sediment diameter. This results in potentially large errors for both the flow problem (actual shear stress) and the sediment diameter. Due to this the availability of hydrodynamic observations at high resolution over a bed of mixed sediments may represent an important step ahead in the present state of the art particularly for accelerated flows such as those under wind generated waves. The uncertainties related to spatial variability will not be properly addressed with flume observations, inevitably limited in size, but the rest of parameters of the flow problem and the sediment problem will be much better controlled.

The distortions due to reflections from flume walls or measuring equipment may also affect the obtained results. Similarly the observed hydrodynamics and morphodynamics may not be (in the long term) in a stable equilibrium which further complicates the problem since there will be a continuous incipient motion affecting potentially the observations.

On the other hand, high resolution observations for hydrodynamics closer to the sea bed thanks to the new advances in high resolution acoustic profilers, may provide an unprecedented dataset that should allow application of a differential treatment for each of the sediment sizes and therefore an improvement over the present state of the art.

2.6 EXPERIMENTAL BACKGROUND

Most of studies previously done dealing with mixed sediment transport consider the study of mixed sediment between sand/mud, sand/gravel or sand/shingles (Sambrock et al. 1997, Blewett et al. 2001, Mason and Coates 2001, San Román-Blanco et al. 2006) and there are just a really limited number of studies, up to the authors knowledge, that deal with different mixtures of different size sands.

Mixed beaches, sand and gravel, are mainly studied from the view point of nourishments or recharge on shingle beaches, which when requiring sediment for nourishment is hardly equal to its

original characteristics. Most of this works are centered in the study area of UK and therefore most of the mixed beaches are analysed when considering a mixture of sand and gravel or even shingles.

Quick and Dyksterhuis (1994) considered that the finest fraction of a mixture of sand and gravel determined hydraulic conductivity by means of decreasing the permeability and beach steepness. Whitcombe (1996) present the different behaviour of replenished shingle beaches when compared to a natural shingle beach. As previously presented by Quick and Dyksterhuis (1994), replenished beaches tend to develop a higher steepness around the mean water level. Again this behaviour is attributed to the higher compaction of the sediment and the permeability reduction due to the finer particles. The hydraulic conductivity of the mixed sediment will be closer to that of the fine sediment when the smaller particles fill the gaps of the coarser sediment. This decrease in the conductivity will reduce the energy absorption capacity, due to water infiltration, of gravel beaches. The change in sediment characteristics (proportion of fine sediment, sediment size and sorting) by means of beach nourishments or recharge schemes, alters the groundwater flow characteristics due to a change in the hydraulic conductivity, which Mason and Coates (2001) identified as the most distinctive property which distinguishes a mixed beach. Defra (2003) and San Román-Blanco et al. (2006) presented a set of mixed beaches experiments (sand/gravel) and reported that mixed beaches should be considered as a continuous spectrum in which the sediment type should not be defined by a single size parameter.

Wilcock et al. (2001) in a series of flow discharge experiments with different mixtures of sand and gravel, showed that total transport rates and gravel transport rates depend strongly on sand content within a mixture. For the same flow strength, gravel transport rates increased by orders of magnitude as sand content increased. The effect of sand content on transport rate may be due to its effect on the critical shear stress (by increasing the amount of sand there is a reduction of the critical shear stress) for incipient motion.

The most relevant bimodal sand studies are the ones done by Holmes et al.. 1996, O'Donoghue and Wright 2004 and Hassan and Ribberink 2005.

Holmes et al.. 1996 presented a set of laboratory experiments in order to study the profile evolution of fine sand (d50 = 0.15 mm), coarse sand (d50 = 0.5 mm) and a bimodal mixture (50/50). The study focus on the sediment transport evolution within the swash zone when having different sedimentary characteristics. The main observations state that a mixture of fine and coarser sands affects the sediment transport in the swash zone, bringing the sediment transport of mixed sediments closer to the transport of fine sand than to the transport measured for coarser sediment. Within the swash zone, the fine sand in the mixture seems to destabilize the coarser sand. This facilitates the erosion of coarser sand on the foreshore and on the seaward slope of the bar. The presented data suggests that the mobility of the coarser sand in the mixture is substantially increased due to a greater exposure and a reduction in friction in the presence of fines. The difference in mobility of fine and coarse sand beds are probably controlled by the different movement threshold condition and the difference in the permeability. The bimodal configurations will have a permeability closer to that of the fine sand, therefore both the fine sand and mixed configurations evolve similarly. The permeability seems to be the dominant controlling factor.

Chatelus et al. 1998 or O'Donoghue and Wright 2004 performed different sets of grading sands mixtures at two different oscillatory flow tunnels (Deltares and Aberdeen University). Both data sets

present mixtures of fine and coarse sand, d50 =0.13 and 0.32 mm for Chatelus et al. 1998 experiments while the mixture is of three different sands (d50 = 0.15, 0.28 and 0.50 mm) in O'Donoghue and Wright 2004. All the experiments were done under sheet flow conditions.

Hassan and Ribberink (2005) carried out laboratory experiments under sheet flow conditions with uniform and mixed sands (both bimodal and trimodal), ranging in size from 0.13 to 0.97 mm, although most previous experience with mix sediments comes from fluvial hydraulics, as described in next section.

2.7 EXPERIMENTAL MODELLING MIXED-SEDIMENTS IN FLUVIAL SYSTEMS

Graded sediments influence sediment transport significantly, but only in recent decades laboratory studies concerning sediment mixtures have assumed a greater relevance. Laboratory experiments have shown that when non-uniform sediment conditions are significant, both a selective transport process of size fractions and a vertical sorting profile in the upper layers of the sandy bed it may take place. Hirano (1971) observed such a mechanism in early laboratory studies with graded sediments. He proposed the existence of an 'active layer' to reflect that part of the bed that is exposed to and interacts with the flow, and is thus subject to entrainment and deposition.

Later experiments for sorting processes acting in graded river beds showed that a distinct surface layer (or Hirano active layer) was an oversimplification of reality, and the addition of a bed layer below the active layer was more illustrative of the spotted by experiments. Particularly, Ribberink (1987) observed the influence of relatively deep bed elevations interacting with the flow and being subject to entrainment and deposition less frequently than higher ones. In order to account for the exchange of sediment through occasional deep bedform troughs, Ribberink introduced the concept of an additional bed layer below the active layer, i.e. the exchange layer, in order to account for the effects of the variability in trough elevations. Although from an engineering point of view, it may be useful to continue considering and improving the concept of discrete bed layers with sediment exchange between the active layer and the exchange layer (Ribberink two-layer model), from a physical point of view, recent laboratory observations do not support such an assumption of discrete bed layers, as can be seen from the measured sorting profiles by Blom et al. (2006). For instance, the variation of the bed composition over bed elevations was continuous and does not show sudden transitions. Based on the experimental results from Ribberink (1987), Armanini (1995) was the first to abandon the concept of discrete bed layers.

Focusing on the vertical sorting phenomenon, Blom et al. (2003) carried out detailed experiments by using a mixture composed of three well-sorted grain size fractions. The length and width of the flume's measurement section were 50 m and 1 m, respectively. During the experiments uniform conditions were maintained and the transported sediment was recirculated, so net aggradation or degradation did not occur. The sediment transport consisted solely of bed load transport.

Bedload transport of particles of different sizes and the same density is typically described in terms of particle relative mobility. This different mobility arises from a balance between two effects: (i) purely inertial effects by which coarser grains are more difficult to mobilize than fine particles due to their masses; and (ii) hiding/exposure effects, whereby compared to particles among other similar-sized particles in uniform sediment, coarser grains are easier to move in a mixture and finer grains are harder to move. Experimental observations (e.g. Parker and Klingeman, 1982) showed that these

two effects often give rise to a system where the small particles are more mobile than large particles, subsequently winnowing the top of the bed of some fraction of small particles, armouring the top layer.

Vertical concentration profiles have been also resulted affected by graded sediment conditions. Laboratory observations with graded sands have shown that suspended sand sizes are smaller than the original sand bed, increasing with the height above the bed. This is due to discrimination with respect to entrainment, although once in suspension finer and coarser grain fractions showed similar concentration profiles (Nielsen, 1983).

Flume experiments have also exposed that mixed sediments tend to stabilize the bottom, thus delaying the appearance of bedforms (Foti and Blondeaux, 1995). Within such phenomenon, it has been observed that bedforms which develop in the presence of graded sediments are characterized by longer wavelengths than those consisting of uniform sand. From observations, it is known that the migration of bedform in itself causes sediment to become redistributed over the active elevations of the bed. Avalanching of grains down a bedform lee face results in a downward coursing trend within bedforms (e.g. Allen, 1965). Furthermore, flume experiments have spotted the importance of taking into account the variability in bedform geometry in modelling sorting and morphodynamics. The work by Paola and Borgman (1991) and Leclair et al. (1997) supports this finding by underlining the impact of the irregularity in bedform size on the formation of sedimentary deposits.

Bimodal sediment mixtures in flume experiments usually consist of sand sized sediment (D50 < 2 mm) and gravel sized sediment (D50 > 2mm) in different proportions. Bimodal mixtures have been used for modelling the effects of sediment sorting processes such as downstream fining (e.g. Paola et al., 1992) and the gravel sand transition (Sambrook-Smith and Ferguson, 1996) and to estimate transport rates where local size information is insufficient to resolve the transport rate on a fraction by fraction basis (Wilcock, 1998). Particularly, Wilcock (1998) by using mixtures of sand and gravel showed that the transport rates of sand and gravel depend on the proportion of each size fraction present in the bed which controls the availability of each size fraction. However, the critical shear stress required to transport the gravel-sized fraction also decreases as the sand content of the mixture increases.

Sambrook-Smith and Ferguson (1996) reported flume experiments with a bimodal gravel/sand and sediment feed, designed to investigate river channel response to declining slope. In their experiments, slope reduction led to immediate increase in depth and reduction in velocity and shear stress, hence progressive aggradation. Deposition was size-selective and led to the following sequence of bed texture change with increasing severity of slope reduction: (i) sand in lee of gravel clusters, (ii) elongated sandy patches and thin streaks, (iii) wider sand ribbons covering gravel completely and developing ripples. There was feedback from the gradual bed surface changes to hydraulic conditions: near-bed velocity increased, while depth, shear stress, and roughness height decreased. These results support the view that the gravel-sand transition along river channels with a local base level control is assisted by positive feedback between changes in bed surface texture and near-bed flow. In addition, Sambrook-Smith and Ferguson (1996) identified that Froude scaling of mixed gravel/sand sized sediment can be problematic, and that scaling all the grain-sizes in a widely-graded mixture at a small geometric scale might result in the finest grains exhibiting cohesive

properties. By introducing hydraulic distortion conditions (by using lower depths and higher slopes to achieve equivalent shear stresses) it would be possible to maintain grain Reynolds numbers indicative of fully rough turbulent flow.

Both bed load and suspended load result in size selective transport and thus contribute to downstream fining under sediment mixture conditions. Viparelli et al. (2010) performed detailed laboratory experiments with a poorly-sorted sand-gravel mixture in a water-feed, sediment-recirculating flume, to characterize the vertical and streamwise grain size structure of the deposit emplaced by an aggrading stream carrying a wide range of sediment sizes. Nine different conditions of equilibrium were reached using different values of water discharge and water surface elevation at the downstream flume end. These experiments allowed for the characterization of (i) a lower regime plane bed equilibrium transport of mixtures of pea gravel and sand, (ii) the evolution towards equilibrium as well as the equilibrium steady state, in terms of measurements of the evolution of the bed profile and of the grain size distribution of the bed surface, and (iii) the creation/consumption of stratigraphy under non-equilibrium conditions (bed aggradation/degradation). The collected data set allowed the testing of existing and new morphodynamic models for lower regime plane bed with non-uniform sediment.

Viparelli et al. (2015) performed an experimental study of the transport of mixtures of particles of differing density in a sediment-feed flume. Sorting and selective transport of particles by material density is important for understanding a wide range of processes, including the formation of mineral placers, deposition of mine tailings and routing of tracers and contaminants. Viparelli et al. (2015) results showed two sorting processes: (i) longitudinal sorting characterized by preferential deposition of heavy particles in the upstream part of the deposit– downstream lightening; and (ii) vertical sorting with less dense particles preferentially deposited in the lowermost portion of the migrating front - upward heavying. Downstream lightening is the analogue of the well-known downstream fining observed in the more studied case of mixtures of heterogeneous size with the river engineering community.

In order to improve our knowledge about the mixed sediment behaviour at hydraulic facilities, the next set of experiments have been planned within the different installations that are part of Hydralab + under the COMPLEX (Cross disciplinary Observations of Morphogynamics and Protective structures, Linked to Ecology and eXtreme events) Joint Research Activity.

3 MIXED SEDIMENTS UNDER RIPPLE REGIME CONDITIONS

The data set out in this study is obtained at the Canal d'Investigació i Experimentació Marítima (CIEM) at the Universitat Politècnica de Catalunya (UPC), Barcelona. It is a large-scale wave flume of 100 m in length, 3 m in width and 4.5 m in depth. The profile used (Figure 1) is characterized by an initial flat profile along 34 m followed by a concrete 1/10 slope for 20 m that ends in a flat concrete section at the same level as the study area. The study section is a sandpit which has a total length of 14 m, followed by a rigid beach profile with a slope of 1/13 for 10 m that ends at an elevation of 0.42 m over the mean water level. The profile ends with a milder section of 2.5 m in order to dissipate the remaining run-up. The mean water level at the toe of the wave paddle is 2.65 m, which produce a water depth in the sandpit of 1 m.

The experiments developed to study the ripple formation within the ripple regime at the CIEM flume is be developed in two phases. The first phase is going to use pure unimodal sediment with a d50 = 0.25 mm enclosed in a sandpit as presented in Figure 1. Within the second phase of the study, part of the fine sediment will be removed from the study area and replaced by coarser sediment with a d50 = 0.54 mm.

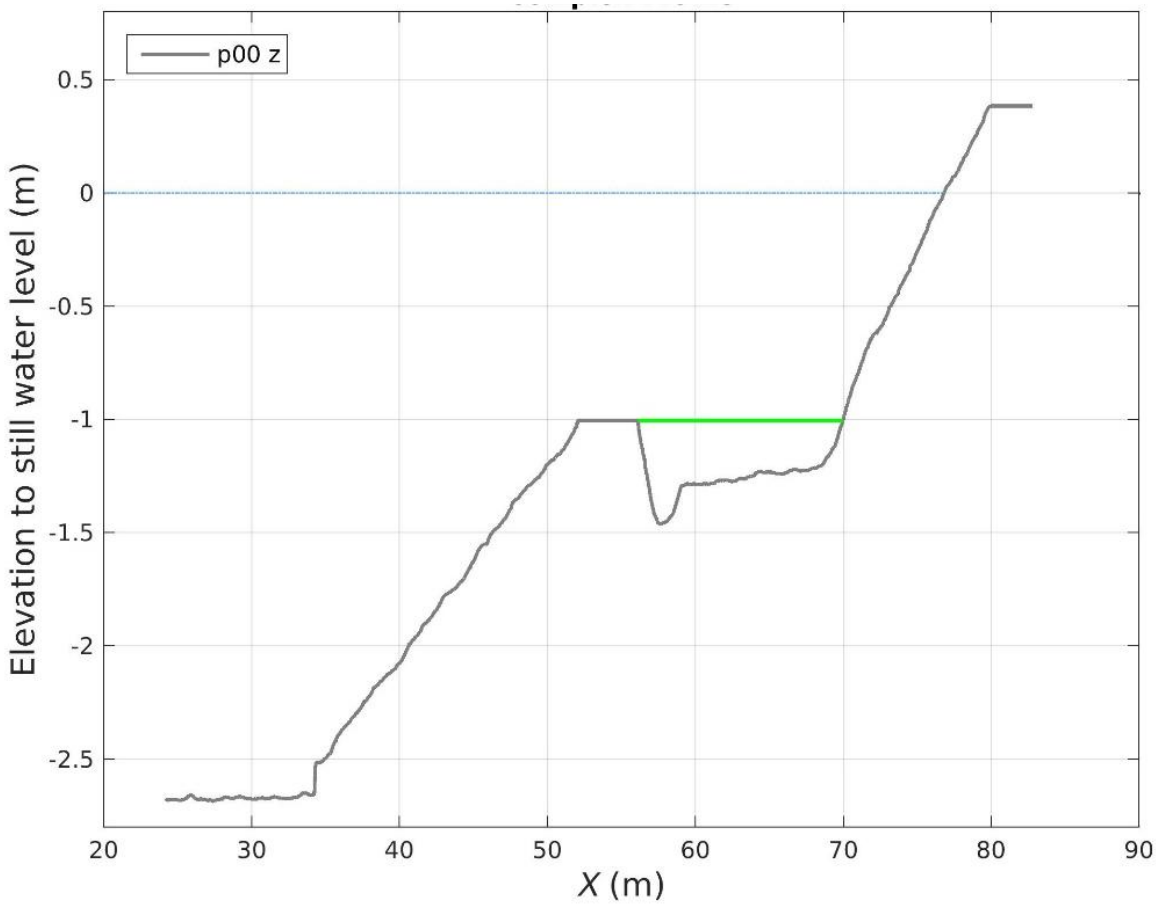

Figure 1: Profile for the flat mixed sediment at the CIEM. In grey rigid bed sections in green movable bed section. The initial flat rigid concrete section has a total length around 5 m, while the (green line) movable bed section has a length around 14 m and includes a total sediment budget of 11 m3 with an average depth of 0.27 m

3.1 RIPPLE FORMULATIONS

Pedocchi and García (2009) and Nelson et al. 2013 comprise best data collections of previous data sets related to ripple studies in the past years. Nelson et al. 2013 collected the wider data set found dealing with ripple studies. They computed 53 different data sets from which 34 % were field data, 32 % Oscillating Water Tunnel experiments, 26 % flume experiments and 8 % others (including basin and flume/tray experiments). Most of the wave flume experiments involved small-scale flume experiments (e.g. Van Rijn 1993, Faraci and Foti 2001, ...) while just three have been done in large scale flumes (Sakakiyama et al. 1986, Williams et al. 2004, Brown 2006). Ruessink et al. 2015 also did large-scale experiments including ripple analysis during the BARDEX data set in the Delta flume, but this experiment was conducted after their publication and therefore is not referred in it.

The authors have found information from three of the four data sets dealing with ripples at large-scale flumes.

- Williams et al. 2004 did a set of experiments produced in the Delta flume where the test section was at a water depth between 4 and 4.5 m. The d_{50} of the experiments tested were 0.162, 0.22 and 0.329 mm, and the ripples had a maximum length of 0.9 m and height of 0.07 m for the 0.162 mm sand configuration. The maximum height and length of the obtained ripples for the 0.22 mm sand tests were 0.02 and 0.65 m respectively. The main difference of this data set to the experiments here planned is the large water depth that Williams et al. 2004 used on their study, where h was around 4 m. Each tests build up from the bottom configuration of the previous wave condition and direct measurements were taken for ripple parameters but not for wave orbital diameter or velocity values. Maximum measured ripple height along the presented experiments is up to 0.02 m for d_{50} = 0.22 mm.
- Brown (2006) presented some of the CROssTEx experiments with non-breaking waves. These experiments present several tested wave conditions (most of them with random wave conditions TMA with H_s between 0.3-0.6 m and T_p between 4-8 s). d_{50} = 0.22 mm. The water depth at the measurement locations is 1.62 and 1.72 m. The experiments used wave time series of 20 minutes and there is no mention of flattening the bed after each experiment, therefore it is assumed that the experiments build up from previous bottom evolution. During this experiments the measured ripples had a maximum ripple height of 0.02 m (TMA: H_s = 0.4 m, T_p = 8 s).
- Ruessink et al. (2015) present data of the BARDEX II experiment. The sediment size has a d_{50} = 0.43 mm and random wave conditions were tested in a study area with a water depth ranging between 1.75 and 3.75 m.

Wave-induced boundary layer streaming produced by the waves progressing over a finite water depth (bottom friction plus wave action) and initially described by Longuet-Higgins (1953) together with the undertow current produced by the Stokes drift are the main difference between the sediment transport experiments done in an Oscillatory water tunnels and a wave flume. Despite these differences, due to the lack of large wave flume experiments with ripples, the best available information to compare our results is found on OWT experiments.

Oscillating water tunnels are able to produce fully turbulent oscillatory flows with velocities and periods that in most cases are greater than what can be achieved in a wave flume, even for the larger installations. On the other hand, the oscillatory motion produced in a U-tunnel produce a constant velocity along the water column and therefore there is lack of the wave streaming produced by the vertical momentum exchange between the free stream and the wave boundary layer.

Kranenburg et al. (2010) describe how the presence of orbital velocities in wave flumes also contribute to increase the onshore transport rates in a wave flumes by vertical advection of sediment. At the end of the onshore/offshore phase of the horizontal orbital velocity, the vertical orbital motion is downward/upward, which causes the sediment to settle faster/slower. The effect is a decrease of transport during the offshore phase and an increase of transport during the onshore phase of the wave.

The wave boundary layer streaming can also be produced by asymmetric waves, as described Ribberink and Al-Salem (1995) or Scandura (2007). This streaming is related to the time variation of turbulence under steady flows (Trowbridge and Madsen, 1984)

O'Donoghue et al. 2006 summarized the state of the art of previous sand ripples research done and added to the existing literature the ripple bed sediment transport experiments performed at the oscillatory flow tunnels of Aberdeen and Delft. It can be understood from his work that sand size is the primary factor determining whether equilibrium ripples will be 2D or 3D. 2D ripples occur when the sand $d_{50} > 0.3$ mm and 3D ripples occur when $d_{50} < 0.22$ mm (except for very low d_0 horizontal water particle excursion). The experiments with pure sand in the Barcelona CIEM flume will be done with the ($d_{50} = 0.25$ mm) which is in the middle of the 2D and 3D predictions.

According to Clifton (1976) there can exist symmetric and asymmetric ripples. The symmetric ripples are classified in three types (orbital, suborbital and anorbital ripples) defined by the relations of the ripple wavelength to grain size (d_{50}) and the maximum wave orbital velocity (u_{max}) at a given wave period. Wiberg and Harris (1994) adopted the orbital-suborbital-anorbital terminology proposed by Clifton (1976) to classify the symmetric ripples. Orbital ripples are defined as the ripples whose wavelength is dependent on the wave orbital diameter and independent of the sediment grain size. Anorbital ripples on the other hand are those ripples whose wavelength depends on the grain size (being λ independent of the wave orbital diameter). Semiorbital ripples are those whose which wavelength is a function of both parameters (wave orbital diameter and the grain size).

$$\frac{\delta_w}{\lambda}$$

This is the main parameter appearing in the formulations and that needs to be derived from laboratory data, following Wiberg and Harris to characterize the ripple regime (orbital/suborbital/anorbital) from the computed data.

Ripple steepness is the ratio between the height and wavelength (η/λ), and is it used to describe the ripple configuration. Dingler and Inman (1977) showed that for fine sand near la Jolla, ripple steepness remained at a value of about 0.15 with increasing wave energy until, sheet flow conditions dominate and the ripples disappear.

The following experiments with comparable wave conditions and similar grain sizes have been conducted in OWTs or wave flumes and can be compared with the results that are to be obtained from the CIEM flume experiments:

1. Experiments in the AOFT with d_{50} of 0.22 mm but with R of 0.63. The reported wave conditions produced 3D ripples, being the larger measured ripples (for FR7 and FR10 with T = 7.38 and 10 s respectively) with η = 54 and 31 mm and and λ = 436 and 250 mm. It is worthwhile also to compare the measured velocities at both cases (u_{max} and u_{rms}, listed on table 1) in order to compare the obtained data and correlated the ripples formation with the measured d_0.
2. Pedocchi and Garcia (2009) conducted several oscillatory water tunnel experiments using d_{50} of 0.25 mm.
3. A set of experiments at the Delta 2 flume (Williams et al., 2004 or Thorne et al., 2002) with d_{50} of 0.22 mm with water depth of 4 m. The problem to compare that data set is the great

water depth that we will not be able to reproduce. The ripple dimensions in these conditions are limited and the 2D/3D outputs are not clearly reported for the different tested conditions. There is an important lack of measurements and, most important, of comparable data in order to cross-analyse the data on ripples (d_0, U_* and similar) and driving terms (water depth, wave height and period).

4. Clubb (2001) presented a large set of experiments in the AOFT. The tested conditions included experiments with sediment sizes ranging between 0.18 and 0.44 mm. Experiments number 17, 18 and 19 were done with d_{50} = 0.26 mm and wave periods of 10 and 15 s reporting as a results velocity measurements u_{rms} = 0.34-0.44 m/s and ripple heights from 0.1 up to 0.19 m.

Nelson et al., 2013 as state of the art paper to consider the different formulation to predict wave-induced ripples concludes that a representative range of different formulations (Foti and Faracci, Wiberg and Harris, Grasmeijer, Mogridge and Nielse) and possible conditions should be considered. This is the approach followed here, presenting the tests in Figure 2 and Table 1. This summarizes the conditions which report the larger ripples within the set of optimum ripple formation waves to be executed. The prediction of the mobility number and orbital velocities to be considered in these formulations have been obtained by means of linear theory.

MWL	H	T	Uorb		MWL	H	T	Uorb
1	0.15	9	0.23		0.9	0.15	9	0.24
1	0.2	9	0.31		0.9	0.2	9	0.33
1	0.3	9	0.46		0.9	0.3	9	0.49
1	0.4	9	0.62		0.9	0.4	9	0.65
1	0.15	8	0.23		0.8	0.15	9	0.26
1	0.2	8	0.31		0.8	0.25	9	0.43
1	0.3	8	0.46		0.8	0.3	9	0.52
1	0.4	8	0.61		0.8	0.4	9	0.69
1	0.15	7	0.23					
1	0.2	7	0.3					
1	0.3	7	0.46					
1	0.4	7	0.61					

Table 1: Table computed using linear theory to compute wave orbital velocities. Values for water depth of 1m in the study area and d50 = 0.25 mm.

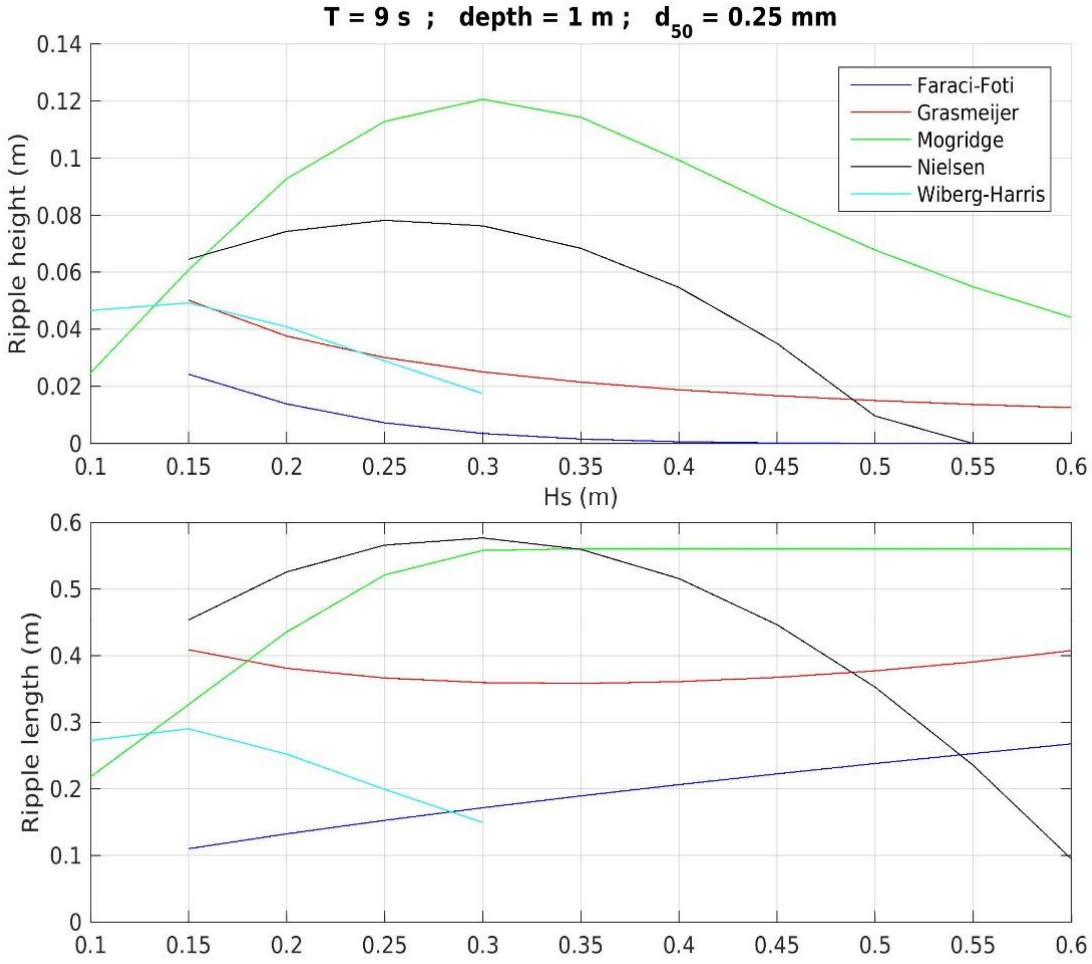

Figure 2: Prediction of ripple height and length when using s-o-a formulations for ripple formation and regime. The water depth of the study area has been fixed for 1m and the presented plot refers to periods of 9 s. The computations have been done using linear wave theory to predict orbital velocities and other parameters requested on the used predictors.

The green colour shows the wave condition for each H, T and MWL that is presented. Mogridge et al. (1994) and Nielsen (1981) formulations are the formulations that predict larger ripples (in height and length). These two formulations were also highlighted by Clubb 2001 as the formulations that present better agreement between measured and predicted ripple lengths under the U-tunnel experiments presented along his work.

Maximum ripples in height and length are obtained for a T of 9 s. Despite that the reflection will also be maximum and therefore it is necessary to assess the wave height distribution along the flume for these conditions and the effect that such reflection will have on the sediment transport patterns. It is to be expected that sediment will accumulate on the antinodes.

For H = 0.3 m and T = 9 s, ripple height should be around 0.12 m and ripple length around 0.6 m, according to Nielsen and Mogridge formulations. The larger the wave period, the larger the forecast of ripple height and length. If we keep increasing T up to 10 s the ripple height increases up to 0.14m.

4 INSTRUMENTATION

The equipment distribution is presented in Figure 3 and Table 2, where the x-coordinate origin is at the wave paddle in resting conditions. The wave height was measured by means of resistive wave gauges in the deeper part of the flume (herein- after WG), pore pressure sensors (PPTs) and acoustic displacement sensors (ADSs). The velocity field was mapped by means of acoustic Doppler velocimeters (ADVs) while optical backscatter sensors (OBSs) are used to recover the suspended sediment concentration (SSC). Two ADVs, the three OBSs and a PPT have been deployed on a custom-built mobile frame (Figure 4). This frame consisted of stainless-steel tubing with 30 mm diameter and was designed such that it would have minimum flow perturbation while being sufficiently stiff to withstand wave impact. The frame was mounted to a horizontally-mobile trolley on top of the flume, and could be vertically positioned with sub-mm accuracy using a spindle. The mobile frame set-up enabled measurements at various cross-shore positions, while maintaining an approximately equal elevation of the instrument array with respect to the bed at the start of each run.

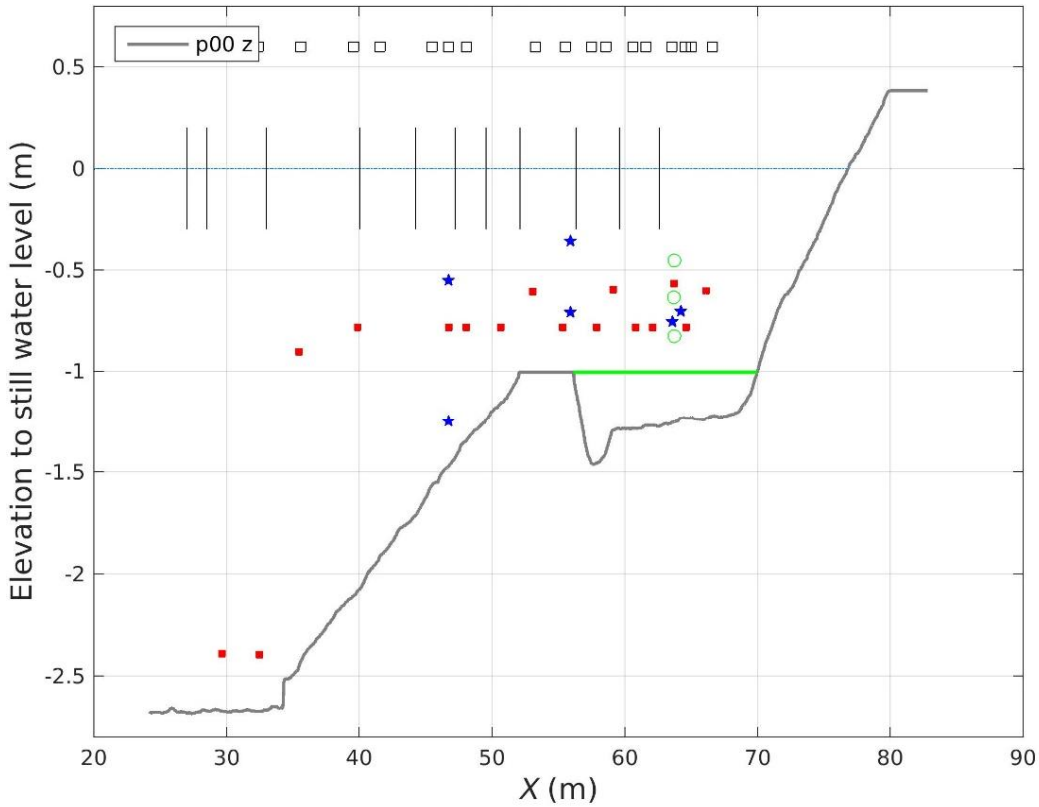

Figure 3: Experimental setup of the Ripcom data set. The solid grey line of the profile presents the rigid bed while the green line present the sediment of the sandpit area. Resistive wave gauges are depicted by black solid lines around the mean water level, Acoustic wave gauges are black upper empty squares, Pressure sensors are presented by red solid squares, ADV measurements are presented by blue pentagrams and empty green circles present the information of OBS locations.

	Cross-shore position (distance to the bottom)
WG	11.84, 27, 28.51, 32.99, 40.02, 44.24, 47.2, 49.56, 52.09, 56.31, 59.59, 62.61
AWG	16.61, 20.71, 23.93, 34.35, 41.54, 45.47, 46.71, 48.07, 53.26, 55.49, 57.47, 58.55, 60.59, 61.58, 63.54, 64.55, 64.98, 66.56,
PPT	29.6 (0.26), 32.44 (0.25), 35.41 (1.7), 39.87 (1.9), 46.71 (1.9), 48.01 (1.9), 50.61 (1.9), 53.04 (2.05), 55.28 (1.9), 57.85 (1.9), 59.08 (2.05), 60.78 (1.9), 62.07 (1.9), 64.58 (1.9), 66.1 (2.05)
ADV	46.71 (1.4), 46.71 (2.1), 55.9 (1.9), 55.9 (2.3)

Table 2: Equipment x and z position along the CIEM flume during the Ripcom experiments. X position has the 0 at the wave paddle in resting conditions while the Z refers to the distance to the bottom, to the concrete bottom of the flume referenced as 0 at the toe of the wave paddle.

Figure 4: Image of the mobile measuring frame instrumentation.

5 INITIAL RESULTS

5.1 UNIMODAL SEDIMENT

As benchmark the sand used on this experiment to build the sandpit is a commercial well-sorted sand with a medium sediment size (d_{50}) of 0.25 mm, with a narrow grain size distribution (d_{10} = 0.154 mm and d_{90} = 0.372 mm) and a measured settling velocity (w_s)of 0.034 m/s.

In accordance to previous computations we should be testing the orbital velocities at the middle of the test section as well as the Sk and As for T = 9 s and H around 0.3 m. We also need to check the wave reflection in front of the wave paddle for all tested conditions. In accordance to previous results our Urms should be within the order of 0.3-0.4 m/s and the orbital excursion should be in the order of 0.6-0.7 m.

So far we have tested several of the planned wave conditions and we have done long runs of experiments for two different wave conditions. We are looking for a balance between the larger periods the possible that produce ripples and the less the possible accumulation of sediment in the antinodes in order to be able to run larger time series and produce the desired ripples.

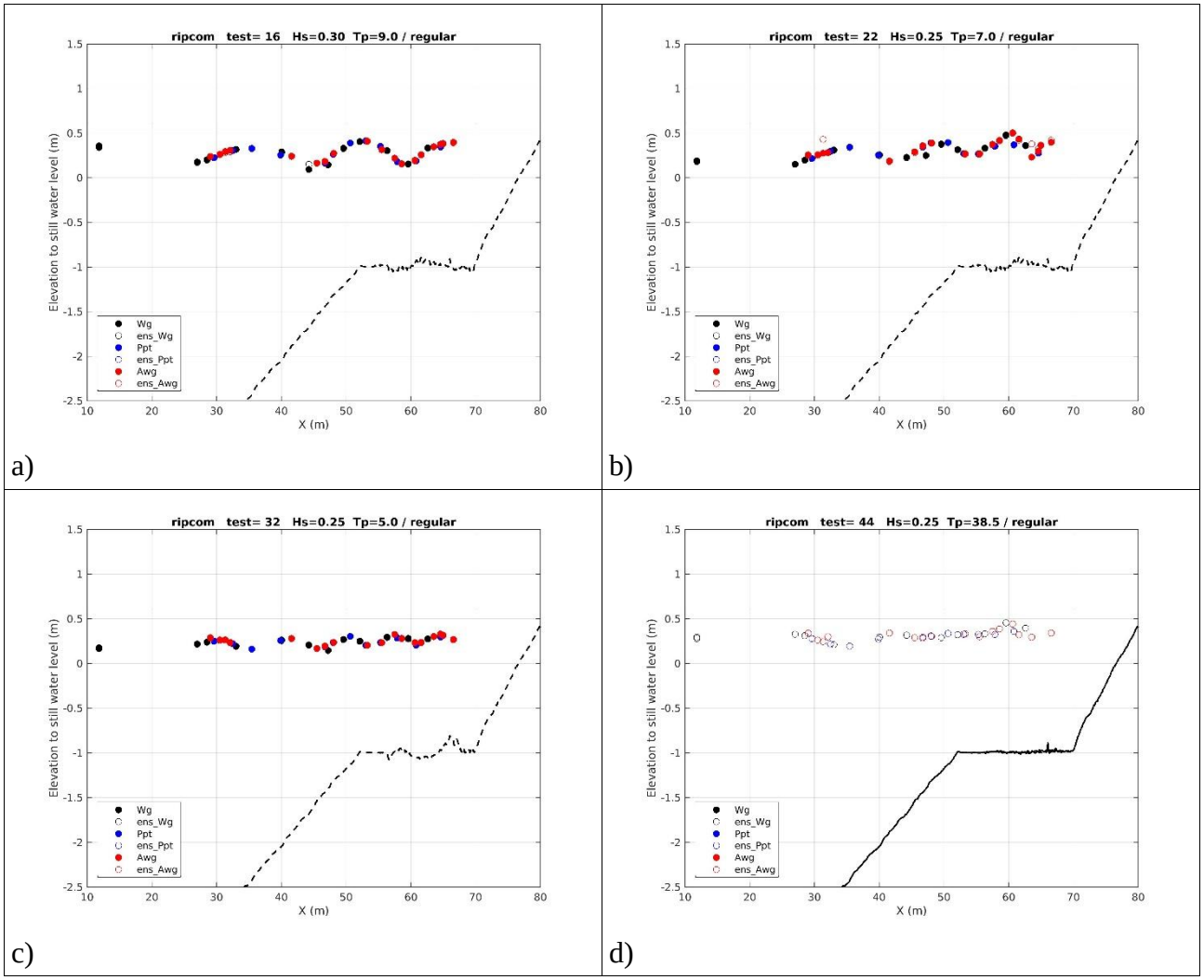

Figure 5: Wave height along the CIEM flume for the different tested conditions M1 (a), M2 (b), M3 (c) and B1 (d). More details of tested conditions can be found on Table 3.

The Reflection analysis performed on the tested conditions is presented at Table 3. Under M1 and M2 (Figure 5-a and b respectively), both conditions produce a high wave reflection and there is a clear sediment accumulation in the antinode within the study area (x around 64 m). This antinode ends by controlling the sediment transport pattern and despite the ripples are generated after some waves there is not enough time to let them evolve without the interference of the megaripple produce by wave reflection

Tested conditions	Reflection (Kr)	
H = 0.3 m, T = 9s M1	0.52	20' (130 waves)
H = 0.25 m, T = 7s M2	0.38	20' (168 waves)
H = 0.25 m, T = 5s M3	0.25	20' (236 waves)
HH=0.25, Tg = 38.5 B1	0.39	f1 = 0.1558, f2 = 0.1299

Table 3: Reflection coefficient for the different tested conditions. B1 tested conditions lasted 20' (31 groups with 2 waves per group) with a total of 62 waves per run.

The generated velocities for the tested conditions are comparable to the velocity measurements previously obtained by Clubb (2001) which ended in ripples. The main difference is the period of tested wave conditions which are importantly lower.

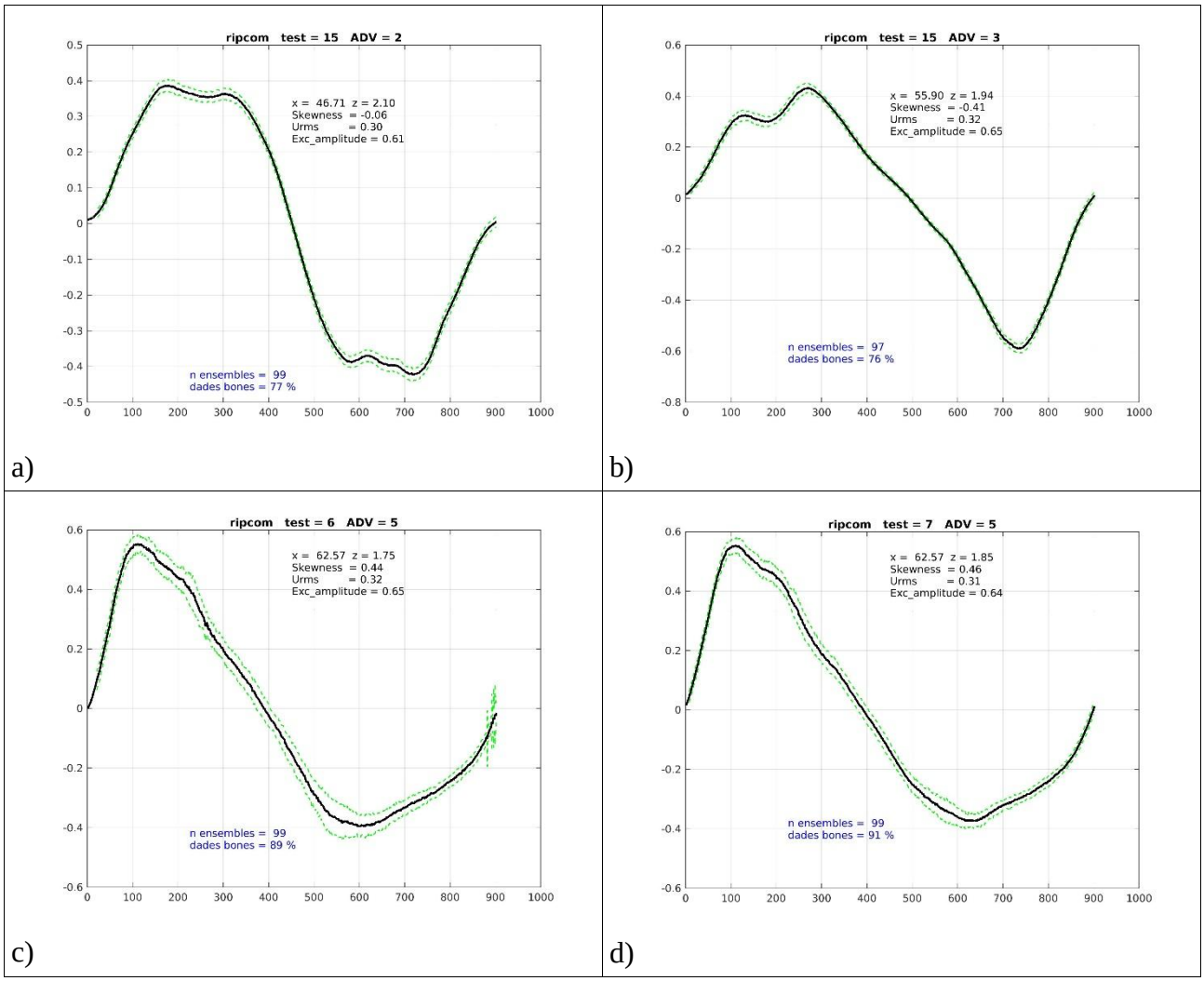

Figure 6: Velocity ensembles for wave conditions (H=0.3 m and T=9 s). In black the Phase average ensemble and in green the standard deviation of all the ensembles used. Figure 6 a) correspond to the velocity at x = 46.7 m along the initial 1/10 slope. Figure 6 b) correspond to the velocity at 55.9 m at the end of the concrete flat part of the profile. Figure 6 c and d) correspond to the velocity computed at the middle of sandpit (x = 62.57 m).

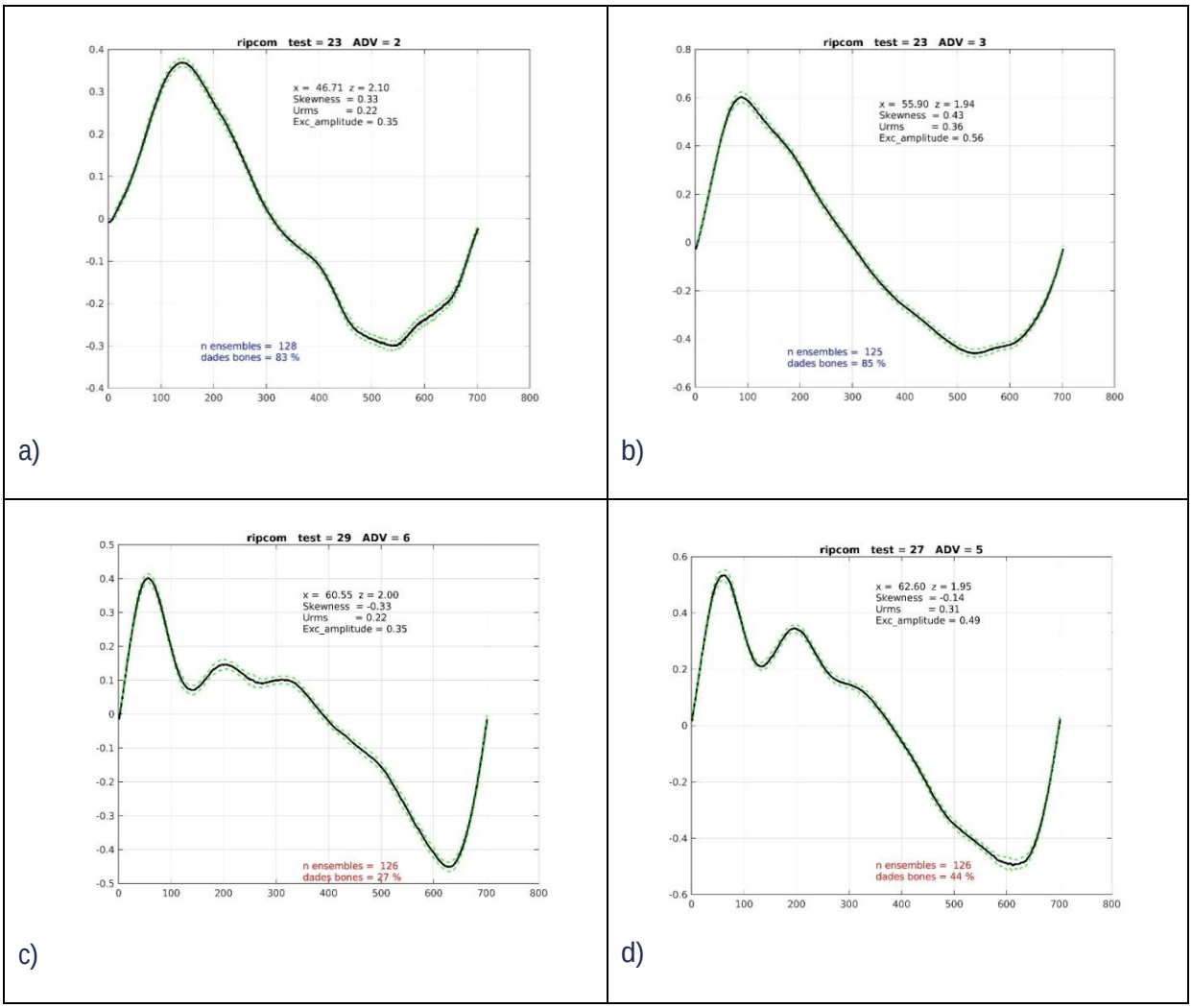

Figure 7: Velocity ensembles for wave conditions (H=0.25 m and T=7 s). In black the Phase average ensemble and in green the standard deviation of all the ensembles used. Figure 7 a) correspond to the velocity at x = 46.7 m along the initial 1/10 slope. Figure 7 b) correspond to the velocity at 55.9 m at the end of the concrete flat part of the profile. Figure 7 c) correspond to the velocity computed at the middle of the sandpit (x = 60.55 m), while Figure 7 d) correspond to the velocity at x = 62.57 m.

All the velocity measurements close or within the sandpit (b, c and d) of Figures 6 and 7 are collected between 20 and 35 cm from the bottom (free stream velocities). The bottom is at 1.65 m from the concrete bottom and the mean water level is at 2.65 m.

5.2 MIXED SEDIMENTS

The sediment to be used in the experiments at CIEM is sand with a grain size d_{50}= 0.545 mm (d_{10}=0.321 and d_{90}=0.794 mm).

In the middle of the testing area a layer of about 25 cm of the mixed sediment will be deployed on top of the original sediment (3 m of fine sediment + 6 m of coarser sediment + 3 m of fine sediment all along flume dimensions).

Within sheet flow conditions a number of authors (O'Donoghue and Wright 2004 a and b; Malarkey and Davies 2009; Ruessink et al.. 2015) present some experiences and describe experiments with

coarser sand with d_{50} of 430 microns. This is being incorporated into the know how to serve for future Hydralab tests combining sediment sizes.

Work undertaken in the Total environment Simulator (TES) flume at the University of Hull using sediments with a D_{50} of 110 µm and 1mm. Experiments were conducted with nine parallel channels 0.48 m wide, 0.2 m high and 7 m long and a10 cm deep sediment substrate. Different treatments were applied to each channel in terms of sediment composition and biofilm growth. Results shown here are for experiments prior to biofilm grown for three channels, one with just fine sediment (110 µm), one with just coarse sediment (1mm) and one with a 50:50 mix of the coarse and fine sediments. Each channel was exposed to unidirectional flow with a mean flow velocity just above the entrainment threshold which resulted in the bedforms shown in Figure 8.

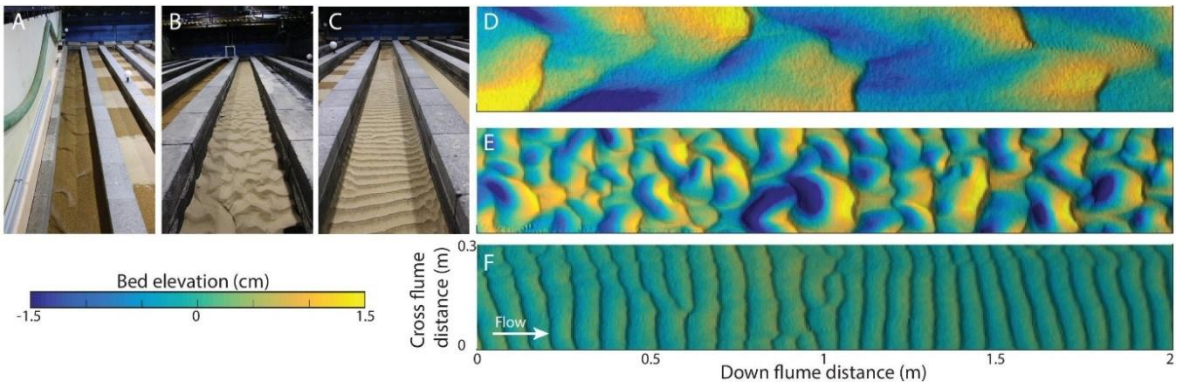

Figure 8: Photographs of channels with coarse (a), fine (b) and mixed (c) sediments. Digital elevation models of the channels with coarse (d), fine (e) and mixed (f) sediments.

The images form each channel show that in both unimodal sediments the bedforms that develop are strongly three-dimensional in terms of their morphology, whilst in contrast the bedforms in the mixed sediment are predominantly two-dimensional in form (Figure 9)

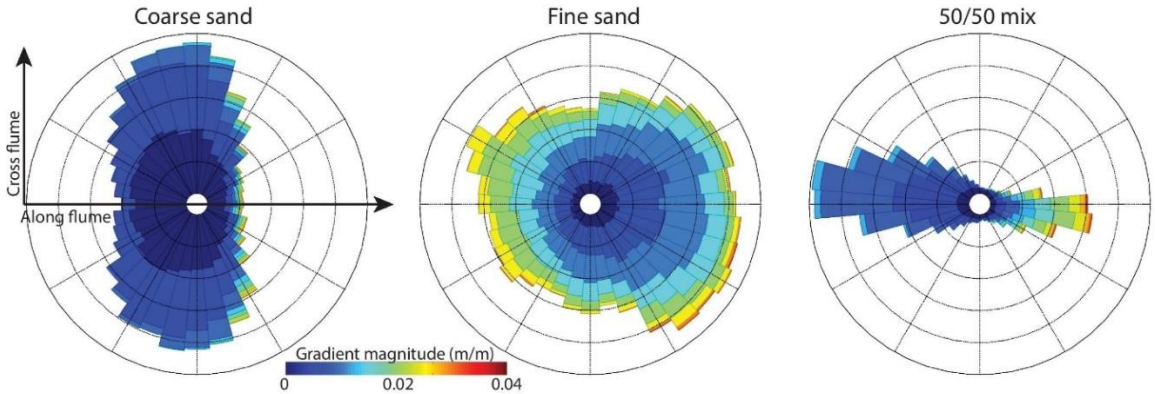

Figure 9: Rose diagrams showing the bed gradient distribution for the Digital elevation model shown in Figure 9 for each of the three channels.

These results show a clear difference in morphology produced by the interaction between different grain sizes. Further work is being undertaken to understand the relationship between the bedform morphology and the flow structure.

5.3 MIXED SEDIMENT UNDER SHEET-FLOW CONDITIONS

Up to date, the transition between ripple and sheet-flow regime has been estimated for uniform sediment only (see section 1.2). To investigate the transition between ripple and sheet-flow regime for mixed sediment as well as the detailed transport processes during the latter, another set of experiments with bimodal sand (D_c = 0.58 mm, D_f = 0.15 mm) will be conducted in the Large Wave Flume (GWK) in Hannover in early 2018. A horizontal bed (30 m length, 5 m width) will be prepared in the middle section of the flume which has a total length of 307 m. Sediment mixtures in this test section will contain different amounts of fine grains (0, 25, 50, 75 and 100 % fines). Two different regular wave conditions will be generated (H1 = 1 m, T1 = 7 s; H2 = 1.5 m, T2 = 7 s): while the first wave condition is used to investigate the transition from ripple development to sheet flow (transition regime), the second condition is expected to provide sheet-flow transport only. If time allows, selected experiments will be repeated with irregular waves. In between the experimental runs with the different wave conditions the bed will be remixed in-situ. Tracer experiments with fluorescent particles and regular sediment samples will allow the study of horizontal and vertical grain movements and size sorting. While the wave characteristics will be measured by the standard GWK instrumentation, further high-resolution instrumentation is used to record the complex flow and sediment transport processes close to the bed:

- ABS suspended sediment concentration
- ACVP flow velocities and sediment concentration profiles
- ADV flow velocities
- CCM+ sheet-flow sediment concentrations and sheet-flow layer thickness
- Ripple profiler acoustic profiling of ripple length and height
- TSS water samples and sediment concentration

The data collected during these unique large-scale experiments are expected to contribute significantly to the understanding of sheet-flow transport of mixed sand and will feed into the development of new numerical tools for the prediction of sediment transport under wave action.

6 CONCLUSIONS

Sediment transport is difficult to predict because of the variety of time and space scales involved and mainly due to the feedbacks with the driving hydrodynamics and resulting bed morphology and evolution, as discussed in the previous sections. It is however important to improve our transport prediction capabilities since they form an essential element in assessing impacts for coastal zones, for instance in terms of erosion or flooding or even the coastal ecosystem evolution.

Mixed sediments involve a significant higher level of complexity due to the a) formulations which are still in its infancy, b) aggregation since the resulting morphodynamic evolution adds in a nonlinear and far for straightforward manner the effects and interactions for each sediment class and c) the

feedbacks. This latter point, as described in the previous part of this deliverable, involves the design of the mixed sediments experiment (scaling, geometry, etc), in terms of the instrumentation (sampling policy and considering the time and space variation of the sediment transport) and finally from the point of view of the interpretation, because of the aforementioned reasons.

The core of the methodology here proposed is based on the necessity to have experimental data under controlled conditions and with limited distortion for engineering analysis and decision making, particularly under future climates. This need is becoming particularly acute under such future scenarios due to the effect of sea level rise that results in coastal zones outside the recent past equilibrium with hydrodynamic drivers and geological settings. The expected acceleration in sea level rise and even our "commitment" to sea level rise beyond 2100 make this necessity urgent and continued, since many of our coastal zones will experience aggravated erosion and flooding problems in the coming decades.

The approach here proposed is intended to demonstrate the feasibility of large scale hydrodynamic and morphodynamic mobile bed experiments based on a limited area. This concept, applicable to both flumes and basins, facilitates the execution of the mixed sediment tests in terms of cost and time. It also helps circumventing the interpretation problems, due to the spatial variability of transport rates mentioned in previous sections.

The tests performed and described in here show how to design a mobile bed local test under large scale and controlled conditions for the case of the Barcelona flume. This is intended to serve as an example and the scientific production to follow will illustrate the application, demonstrating the use of limited area results for engineering decisions and hydro-morphodynamic modelling. For the time being the presence of sediment mixes, although poorly known in terms of behaviour, is well recognized to be at the core of the hydro-transport-morphological triangle, resulting in different impact predictions as a function of the sediment mix characteristics. The observed over and under predictions of transport rates are now better understood and with the generation of a benchmark dataset within Hydralab+ they will be easier to incorporate in the present state of art modelling and engineering.

REFERENCES

Allen, J. R. L. (1965). Sedimentation to the lee of small underwater sand waves: An experimental study, J. Geol., 73, 95 - 116.

Armanini, A. (1995). Non-uniform sediment transport: Dynamics of the active layer, J. Hydraul. Res., 33(5), 611–622.

Blewett, J.C., Holmes, P., Horn, D.P., 2001. Field Measurements of swash hydrodynamics on sand and shingle beaches. Implications for sediment transport. Coastal Dynamics.

Blom, A., Ribberink, J. and de Vriend, H. (2003). Vertical sorting in bed forms: Flume experiments with a natural and a trimodal sediment mixture, Water Resour. Res., 39(2), 1025.

Blom, A., Parker, G., Ribberink, J. and de Vriend, H. (2006). Vertical sorting and the morphodynamics of bed-form-dominated rivers: An equilibrium sorting model, J. Geophys. Res., 111.

Brown, J.A., 2006. Sea-bed response to non-breaking waves PhD Thesis. The Ohio State University.

Chatelus, Y., Katopodi, I., Dohmen-Janssen, M., Ribberink, J.S., Samothrakis, P., Cloin, B., Savioli, J.C., Bosboom, J., O'Connor, B.A., Hein, R. and Hamm, L., 1998. Size gradation effects in sediment transport. International Conference on Coastal Engineering, 2345-2448.

Church, M.; Hassan, M. A. 2002. Mobility of bed material in Harris Creek, Water Res. Res. 38(11):1237. doi:10.1029/2001WR000753.

Clifton, H.E., 1976. Wave-formed sedimentary structures: A conceptual model. Beach and Nearshore Sedimentation, Richard A. Davis, Jr., Raymond L. Ethington. SEPM Society of Sedimentary Geology Vol 24, 126-148.

Clubb, G.S., 2001. Experimental study of vortex ripples in full scale sinusoidal and asymmetric flows. PhD Thesis. University of Aberdeen.

Defra, 2003. Development of Predictive Tools and Design Guidance for Mixed Beaches, Stage 2. Food and Rural Affairs Final Project Report FD1901. Department of Environment, London.

Dingler, J. R., and Inman, D. L. 1977. Wave-formed ripples in nearshore sands. Proceedings of the 15th Coastal Engineering Conference, vol. 2, pp. 2109–2126, New York, USA.

Eidsvik, K.J. Some contributions to the uncertainty of sediment transport predictions. Continental Shelf Research 24 (2004) 739–754.

Faraci, C. and Foti, E., 2001. Evolution of small scale regular patterns generated by waves propagating over a sandy bottom. Physics of Fluids, Vol. 13 (6), 1624-1634.

Foti, E. and Blondeaux, P. (1995). Sea ripple formation: the heterogeneous sediment case. Coastal Engineering, 25, 267-253.

Hassan, W.H. and Ribberink, J.S., 2005. Transport processes of uniform and mixed sands in oscillatory sheet flow. Coastal Engineering, 52, 745-770.

Hirano (1971). River bed degradation with armouring. Trans. Japan. Society of Civil Engineers, 195, 55-65.

Holmes, P., Baldock, T.E., Chan, R.T.C. and Neshaei, M.A.L., 1996. Beach evolution under random waves. 25th Int. Conf. Coastal. Eng. Orlando, USA, 3006-3019.

Iseya, F. and Ikeda, H., 1987. Pulsations in bedload transport rates induced by a longitudinal sediment sorting: A flume study using sand and gravel mixtures. Geografiska. Annaler. 69 A (1):15

Komar P.D. and Li Z. 1988. Applications of grain pivoting and sliding analyses to selective entrainment of gravel and to flow competence evaluations. Sedimentology, 35, 681– 95.

Kostaschuk, R., Bestb, J., Villardc, P., Peakallb, J. and Franklin, M. Measuring flow velocity and sediment transport with an acoustic Doppler current profiler. Geomorphology 68 (2005) 25–37.

Kranenburg, W., Ribberink, J. and Uittenbogarrd, R., 2010. Sand transport by surface waves: Can streaming explain the onshore transport?. 32nd International Conference on Coastal Engineering, Shanghai, China.

Leclair, S., Bridge, J.and Wang, F. (1997). Preservation of cross-strata due to migration of subaqueous dunes over aggrading and non-aggrading beds: Comparison of experimental data with theory, Geosci. Can., 24, 55–66.

Longuet-Higgins, M. S., 1953. Mass transport in water waves, Philos. Trans. R. Soc. London, Ser. A, 245, 531–581.

Mason, T., Coates, T.T., 2001. Measuring and modelling sediment transport on mixed beaches: a review. Journal of Coastal Research 17 (3), 645–657.

Mogridge, G. R., Davies, M. H., and D. H. Willis, 1994. Geometry prediction for wave-generated bedforms. Coastal Engineering, Vol. 22(3), 255–286.

Nelson, T.R., Voulgaris, G. and Traykovski, P., 2013. Predicting wave-induced ripple equilibrium geometry. Journal of Geophysical Research, Vol. 118, 3202-3220.

Nielsen, P., 1981. Dynamics and geometry of wave-generated ripples. Journal of Geophysical Research, Vol. 86(C7), 6467–6472

Nielsen, P. (1983). Entrainment and distribution f different sand sizes under water waves. J. Sed. Pet., 53(2), 423-428.

O'Donoghue, T. and Wright, S., 2004. Flow tunnel measurments of velocities and sand flux in oscillatory sheet flow for well-sorted and graded sands. Coastal Engineering, 51, 1163-1184.

O'Donoghue, T., Doucette, J.S., van der Werf, J.J., Ribberink, J.S., 2006. The dimensions of sand ripples in full-scale oscillatory flows. Coastal Engineeringm, Vol. 53, 997–1012.

Parker G., and Klingeman P.C., 1982. On why gravel bed streams are paved. Water Resources Research, 18, 1409–1423. doi:10.1029/WR018i005p01409.

Paola, C., and Borgman, L. (1991). Reconstructing random topography from preserved stratification. Sedimentology, 38, 553–565.

Parker, G. and Klingeman, P. (1982) On why gravel bed streams are paved. Water Resour. Res., 18, 1409 -1423.

Pedocchi, F. and Garcia,M. H., 2009. Ripple morphology under oscillatory flow: 2. Experiments. Journal of Geophysical Research, Vol. 114, C12015.

Quick, M.C., Dyksterhuis, P., 1994. Cross-shore transport for beach of mixed sand and gravel. Proceedings of the International Sympo- sium on Waves, Physical and Numerical Modelling. IAHR, Vancouvert, 1443–1452.

Ribberink, J. S., and Al-Salem, A. A., 1995. Sheet flow and suspension of sand in oscillatory boundary layers, Coastal Engineering, Vol. 25, 205-225.

Ruessink, G., Brinkkemper, J.A., and Kleinhans, M.G., 2015. Geometry of wave-formed orbital ripples in coarse sand. Journal of Marine Science and Engineering, Vol. 3, 1568-1594.

Sakakiyama, T., T. Shimizu, R. Kajima, S. Saito, and Maruyama, K., 1986. Sand ripples generated by prototype waves in a large wave flume, Coastal Eng. Jpn., 28, 147-160.

San Román-Blanco, B.L, Coates, T.T., Holmes, P., Chadwick, A.J., Bradbury, A., Baldock, T.E., Pedrozo-Acuña, A., Lawrence, J. and Grüne, J., 2006. Large scale experiment on gravel and mixed beaches: Experimental procedure, data documentation and initial results. Coastal Engineering, 2006, 349-362.

Sambrook-Smith, G. and Ferguson, R. (1996). The gravel-sand transition: Flume study of channel response to reduced slope. Geomorphology, 6(2), 147-159.

Sambrock, G.H., Nicholas, A.P. and Ferguson, R.I., 1997. Measuring and defining bimodal sediments: Problems and implications. Water Resources Research, Vol. 33, No. 5, 1179-1185.

Thorne, P.D. and Hanes, D.M., 2002. A review of acoustic measurement of small-scale sediment processes. Continental Shelf Research, 22(4): 603-632.

Thorne, P.D., Williams, J.J. and Davies, A.G., 2002. Suspended sediments under waves measured in a large-scale flume facility. Journal of Geophysical Research, Vol. 107 (C8),

Trowbridge, J., and Madsen, O. S., 1984. Turbulent wave boundary layers: 2. Second-order theory and mass transport, J. Geophys. Res., 89, 7999–8007.

Van Rijn, L.C., Nieuwjaar, M.W., van der Kaay, R., Nap, E. and van Kampen, A., 1993. Transport of fine sands by currents and waves. Journal of Waterway, Port, Coastal, and Ocean Engineering. 119(2), 123-143.

Viparelli, E., Haydel, R., Salvaro, M., Wilcock, P. R., and Parker, G. (2010). River morphodynamics with creation/consumption of grain size stratigraphy 1: laboratory experiments. J. Hydraul. Res., 48, 715 -726.

Viparelli, E., Solari, L. and Hill, K. (2015). Downstream lightening and upward heavying: Experiments with sediments differing in density, Sedimentology. 62, 1384–1407.

Wheaton, J.M., Brasington, J., Darby, S.E. and Sear D.A. (2010) Accounting for uncertainty in DEMs from repeat topographic surveys: improved sediment budgets. Earth Surf. Process. Landforms 35(2), 136–156.

Whitcombe, L.J., 1996. Behaviour of an artificially replenished shingle beach at Hayling Island, UK. Quarterly Journal of Engineering Geology 29 (4), 265–271

Wiberg, P.L. and Harris, C.K., 1994. Ripple geometry in wave-dominated environments. Journal of Geophysical Research, Vol. 99 C1, 775-789.

Wilcock, P. (1998). Two-fraction model of initial sediment motion in gravel-bed rivers. Science, 280(5362), 410-412.

Wilcock, P. R., Kenworthy, S. T., and Crowe, J. C., 2001. Experimental study of the transport of mixed sand and gravel. Water Resources Research, 37, nº 12, 3349-3358.

Wilcock, P., Pitlick, J. and Cui, Y. Sediment Transport Primer Estimating Bed-Material Transport in Gravel-bed Rivers. USDA Forest Service, Rocky Mountain Research Station. General Technical Report RMRS-GTR-226 (2009).

Williams, J. J., Bell, P. S., Thorne, P. D., Metje, N., and Coates, L. E., 2004. Measurement and prediction of wave-generated suborbital ripples, Journal of Geophysical Research, Vol. 109.